Effect of an applied magnetic field on interface excitations in finite layered structures. III

Manvir S. Kushwaha
Departamento de Física, Instituto de Ciencias, Universidad Autónoma de Puebla, Apartado Postal J-48, Puebla 72570, Mexico
(Received 9 September 1987; revised manuscript received 9 November 1988)

The interface excitations associated with double inversion layers in a finite semiconductor-insulator-semiconductor structure are investigated. The layered structure is assumed to be subjected to a magnetostatic field ($\mathbf{B}_0$) applied parallel to the direction of propagation and to the interfaces (Faraday configuration). The exact dispersion relation which governs the propagation characteristics of two-dimensional charge carriers under the influence of an applied magnetic field has been derived on the basis of local theory. The model the author has developed is sufficiently realistic in that it does not ignore the three-dimensional effects in the bulk semiconductor layers. The general dispersion relation which is found to be size dependent and a function of the dielectric properties of the constituent layers has been solved numerically, without any restrictions. The exact numerical results demonstrate the dependence of the coupled modes of excitations on the insulator thickness and the size of the structure. The dispersion characteristics have been discussed in light of recent work in other configurations.

The drive to develop exotic multicomponent solid-state devices is increasing the need to understand inversion layers on semiconductors. Although the existence of Wigner crystallization of two-dimensional (2D) electrons had been anticipated for so many years, the pioneering work by Fowler *et al.*[1] really established the 2D character of inversion layers. The most distinctive excitations of a 2D electron-gas system are 2D plasma oscillations. This is because, contrary to its 3D analog, the 2D plasmon dispersion relation starts at the origin. The existence of 2D plasmons was first predicted theoretically by Stern,[2] and since then the subject has received considerable attention for different possible geometries.[3–10]

Recently, the present author has embarked on a systematic study of the effect of an applied magnetic on the interface excitations associated with the double inversion layers of a finite *p*-type semiconductor–insulator–*n*-type semiconductor (SIS) structure with perfectly conducting (metallic) sheets (Fig. 1). The motivation behind the choice of such structures was the possibility of their practical realization in the laboratory. On the basis of the theoretical model within the local approximation, we investigated and predicted the dependence of the coupled magnetoplasma modes on the insulator thickness and the size of the layer SIS structure in the perpendicular and the Voigt configurations.[11,12] References 11 and 12 hereinafter will be referred to as I and II, respectively.

In the present work we concentrate on the interface excitations of a finite SIS structure subjected to an applied magnetic field in the Faraday configuration. It should be pointed out that our accomplishment lies in investigating the effect of the insulator thickness and the size of the structure on the behavior characteristic of the coupled magnetoplasma interface excitations in a finite layered SIS structure.

In Fig. 1 we show the model structure. The region A ($-D<z<-d$) is an *n*-type semiconductor, region B ($-d<z<d$) is an insulator, and region C ($d<z<D$) is a *p*-type semiconductor. We assume the outer surfaces of the structure to be coated with perfectly conducting (metallic) sheets which provide the grounding of the tangential components of electric fields at $z=\pm D$. This results in the suppression of the electromagnetic surface waves which would otherwise be present at the plasma-vacuum (outer) boundaries. From an analytical point of view, this simplifies the mathematical complexity considerably. Furthermore, we assume that 2D *p*-type and *n*-type inversion layers exist, respectively, at *A*-*B* and *B*-*C* interfaces. The 2D inversion layers have the polarizability tensor $\tilde{\chi}^A$

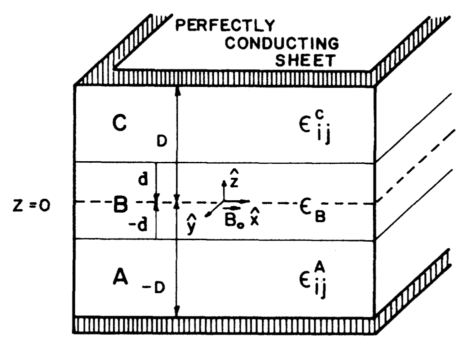

FIG. 1. The schematic illustration of a semiconductor-insulator-semiconductor structure with perfectly conducting (metallic) sheets. A 2D electron gas and a 2D hole gas are assumed to exist, respectively, at *B*-*C* and *A*-*B* interfaces. The applied magnetic field $\mathbf{B}_0 \| \hat{\mathbf{x}}$ is oriented parallel to the direction of propagation and to the interfaces (Faraday geometry).

and $\tilde{\chi}^C$, where superscripts A and C refer, respectively, to the A-B and B-C interfaces. This implies that an electric field of the form $E(z)e^{i(q_x x-\omega t)}$ evaluated at the planes $z=\pm d$ will cause the polarization of the 2D electron gas (at $z=+d$) and of 2D hole gas (at $z=-d$) of the form $\mathbf{P}(\mathbf{r},t)=[P_x(q,\omega),P_y(q,\omega)]\delta(z\pm d)$, where $\mathbf{P}(q,\omega)=\tilde{\chi}(q,\omega)\cdot\mathbf{E}$. The polarizability tensor $\tilde{\chi}$ and the conductivity $\tilde{\sigma}$ are related such that $\tilde{\sigma}=-i\omega\tilde{\chi}$.

We start with Maxwell's curl field equations (in the cgs system of units). Elimination of the magnetic field variable $\mathbf{B}$ leaves us with the following wave field equation in terms of the macroscopic electric field $\mathbf{E}$:

$$\nabla\times(\nabla\times\mathbf{E})-\frac{4\pi i}{\omega}q_0^2\mathbf{J}-q_0^2\tilde{\epsilon}\cdot\mathbf{E}=0\ , \tag{1}$$

where q_0 $(=\omega/c)$ is the vacuum wave vector. $\tilde{\epsilon}$ is the dielectric function appropriate to the medium in which the wave equation is being applied. $\mathbf{J}(\mathbf{r},t)=\mathbf{J}(q,\omega)e^{i(q_x x-\omega t)}\delta(z\pm d)$ is the current density associated with the respective inversion layers. To be more precise, $\mathbf{J}(q,\omega)=-i\omega\tilde{\chi}(q,\omega)\cdot\mathbf{E}$. For $z\neq\pm d$, the wave equation in the presence of an applied magnetic field ($\mathbf{B}_0\|\hat{\mathbf{x}}$) attains a standard form

$$\begin{bmatrix} q_0^2\epsilon_{xx}-q_z^2 & 0 & q_xq_z \\ 0 & q_0^2\epsilon_{yy}-q_x^2-q_z^2 & q_0^2\epsilon_{yz} \\ q_xq_z & -q_0^2\epsilon_{yz} & q_0^2\epsilon_{yy}-q_x^2 \end{bmatrix}\begin{bmatrix} E_x \\ E_y \\ E_z \end{bmatrix}=0\ . \tag{2}$$

In the situation at hand ($\mathbf{B}_0\|\hat{\mathbf{x}}$), the Cartesian elements ϵ_{ij} of the dielectric tensor ($\tilde{\epsilon}$) simplified by the symmetry requirements are the same as given in the Appendix in II. Equation (2) is a set of three linear homogeneous equations satisfied by the electric field in the dispersive, anisotropic, semiconducting media (regions A and C in Fig. 1). The same set of three equations can also give valid solutions of Maxwell's equations in the isotropic, insulating thin film (region B) under appropriate conditions (viz., $\epsilon_{yz}=0$ and $\epsilon_{yy}=\epsilon_{xx}=\epsilon_B$). This set of equations admits a nontrivial solution if and only if the determinant of the coefficients vanishes. This leave us, after some algebra, with the following relation:

$$-q_z^2=\alpha_\pm^2=\frac{1}{2\epsilon_{yy}}\left(\,[(\epsilon_{yy}+\epsilon_{xx})K^2-q_0^2\epsilon_{yz}^2]\pm\{\,[(\epsilon_{yy}-\epsilon_{xx})K^2-q_0^2\epsilon_{yz}^2]^2-4q_x^2q_0^2\epsilon_{xx}\epsilon_{yz}^2\}^{1/2}\right)\ , \tag{3}$$

where $K^2=q_x^2-q_0^2\epsilon_{yy}$ in the semiconducting media, and

$$-q_z^2=\alpha_B^2=q_x^2-q_0^2\epsilon_B \tag{4}$$

in the insulating medium. In Eqs. (3) and (4), $\alpha_\pm(=\pm iq_z)$ refers to the decay constants in regions A and C, and α_B $(=\pm iq_z)$ to that in region B.

We express the spatial and temporal dependence of the fields in the three media in the form (see Fig. 1), $\mathbf{E}(\mathbf{r},t)=\mathbf{E}(z)e^{i(q_x x-\omega t)}$, where $\mathbf{E}(z)$ in regions A, B, and C assumes the form

$$\mathbf{E}^A(z)=\mathbf{E}_1^Ae^{\alpha_{A+}z}+\mathbf{E}_2^Ae^{-\alpha_{A+}z}+\mathbf{E}_3^Ae^{\alpha_{A-}z}+\mathbf{E}_4^Ae^{-\alpha_{A-}z}\ , \tag{5}$$

$$\mathbf{E}^B(z)=\mathbf{E}_1^Be^{\alpha_Bz}+\mathbf{E}_2^Be^{-\alpha_Bz}\ , \tag{6}$$

$$\mathbf{E}^C(z)=\mathbf{E}_1^Ce^{\alpha_{C+}z}+\mathbf{E}_2^Ce^{-\alpha_{C+}z}+\mathbf{E}_3^Ce^{\alpha_{C-}z}+\mathbf{E}_4^Ce^{-\alpha_{C-}z}\ . \tag{7}$$

Note that analogous solutions can be written for the magnetic field variable $\mathbf{B}$ in the respective regions.

The determination of the dispersion relation for interface excitations in the configuration at hand requires that the fields must satisfy certain electromagnetic boundary conditions at all the surfaces ($z=\pm D$) and the interfaces ($z=\pm d$). The boundary conditions are the continuity of the tangential electric and magnetic field components (i.e., E_x, E_y, B_x, and B_y) at the two interfaces and the vanishing of the tangential electric fields (i.e., E_x and E_y) at the outer (metallized) surfaces. Making use of Maxwell's curl field equations and Eq. (2), one can express the field components E_x, B_x, and B_y in terms of the E_y component in regions A and C. Similarly, B_x and B_y components in region B can be expressed, respectively, in terms of E_y and E_x. This greatly reduces the number of unknown parameters involved. As such, matching of the fields at the surfaces and interfaces yields the following (implicit) general dispersion relation:

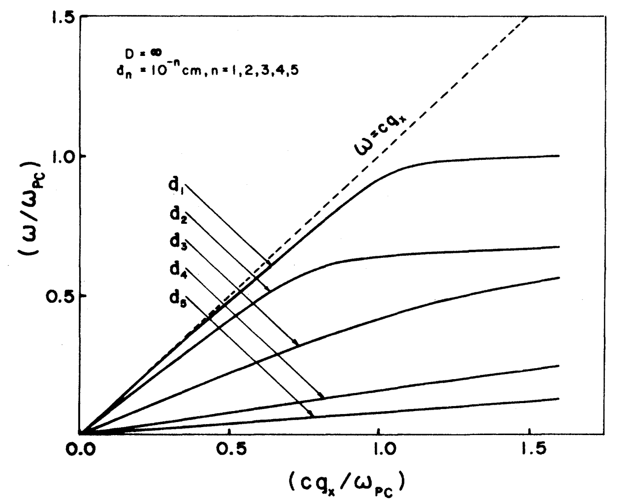

FIG. 2. Dispersion curves for the semi-infinite structure (i.e., $D=\infty$). The modes designated d_1, d_2, and d_3 correspond, respectively, to the three values of insulator thickness as defined in the figure. The dashed line is the light line ($\omega=cq_x$) in the vacuum.

$$\epsilon_B(R_{C_1}R_{A_2}+R_{C_2}R_{A_1})\text{cosech}^2(\theta)+\left[R_{C_3}R_{A_3}+\alpha_B^2R_{C_4}R_{A_4}+\frac{\epsilon_B^2}{\alpha_B^2}R_{C_5}R_{A_5}+\epsilon_B^2R_{C_6}R_{A_6}\right]$$
$$+\epsilon_B(R_{C_3}R_{A_6}+R_{C_6}R_{A_3}+R_{C_4}R_{A_5}+R_{C_5}R_{A_4})\coth^2(\theta)+\left[\left[\frac{\epsilon_B}{\alpha_B}R_{C_5}+\alpha_BR_{C_4}\right](\epsilon_BR_{A_6}+R_{A_3})\right.$$
$$\left.+\left[\frac{\epsilon_B}{\alpha_B}R_{A_5}+\alpha_BR_{A_4}\right](\epsilon_BR_{C_6}+R_{C_3})\right]\coth(\theta)=0\ , \qquad (8)$$

where

$$R_{j_1}=\frac{1}{j_5j_6}(T_{j_-}j_1-T_{j_+}j_2)\left[j_1j_4\frac{T_{j_+}}{\alpha_{j_-}}-j_2j_3\frac{T_{j_-}}{\alpha_{j_+}}\right],$$
$$R_{j_2}=\frac{1}{j_5j_6}(T_{j_+}j_1-T_{j_-}j_2)(T_{j_-}\alpha_{j_+}-T_{j_+}\alpha_{j_-})\ ,$$
$$R_{j_3}=\frac{1}{j_5j_6}\left[j_5j_6-(T_{j_-}\alpha_{j_+}-T_{j_+}\alpha_{j_-})\times\left[j_1j_4\frac{T_{j_+}}{\alpha_{j_-}}-j_2j_3\frac{T_{j_-}}{\alpha_{j_+}}\right]\right],$$
$$R_{j_4}=\frac{1}{j_6}(T_{j_-}j_1-T_{j_+}j_2)\ ,$$
$$R_{j_5}=\frac{1}{j_5}(T_{j_+}j_1-T_{j_-}j_2)\ ,$$
$$R_{j_6}=R_{j_4}R_{j_5}\ ,$$

where $j_1=\alpha_{j_+}j_+$, $j_2=\alpha_{j\_}j_-$, $j_3=\epsilon_{j_+}j_1$, $j_4=\epsilon_{j\_}j_2$, $j_\pm=iq_x(K_j^2-\alpha_{j\pm}^2)/[q_0^2\epsilon_{yz}^j(\alpha_{j\pm}^2+q_0^2\epsilon_{xx}^j)]$, $\epsilon_{j_\pm}=(\epsilon_{xx}^j+4\pi\chi_{xx}^j\alpha_{j_\pm})$, $j_5=(j_3/\alpha_{j_+}-j_4/\alpha_{j\_})$, $j_6=(\alpha_{j\_}j_1-\alpha_{j_+}j_2)$, $\theta=2\alpha_Bd$, and $T_{j_\pm}=\tanh[\alpha_{j_\pm}(D-d)]$; $j\equiv C, A$ (Ref. 13). It is found that our general dispersion relation when subjected to the special limits[11,12] reproduces exactly the results previously reported for single-interface and double-interface (semi-infinite and finite) structures with and without an applied magnetic field.[2-10]

The general dispersion relation, Eq. (8), for coupled modes of excitations (CME's) governs the dynamical behavior of 2D inversion layers at the interfaces, and also embodies the 3D effects in the bulk semiconductor layers. For the numerical examples presented here, we specify our SIS structure such that region A is n-type InSb, region B is vacuum (i.e., $\epsilon_B=1$), and region C is p-type InSb. We use the following material parameters: $\epsilon_L=15.7$, $\epsilon_B=1.0$, $\nu=0$, $n_e=2\times10^{12}\ \text{cm}^{-2}$, $m_e=0.2m_0$, and $m_h=0.4m_0$, m_0 being the free-electron mass. The subscripts e and h stand for electron and hole, respectively. The magnitude of $\mathbf{B}_0$ was chosen such that $\omega_{cC}/\omega_{pC}=0.5$, where ω_{cC} and ω_{pC} are, respectively, the cyclotron frequency and the screened plasma frequency in region C (Fig. 1). Note that we have carried out the computation retaining the retardation effect. Furthermore, we have confined our attention to the solutions which decay exponentially away from both interfaces inside the insulator film. Such solutions are characterized by α_B being real and positive. We will be interested in the situation where q_x is real when absorption is neglected.

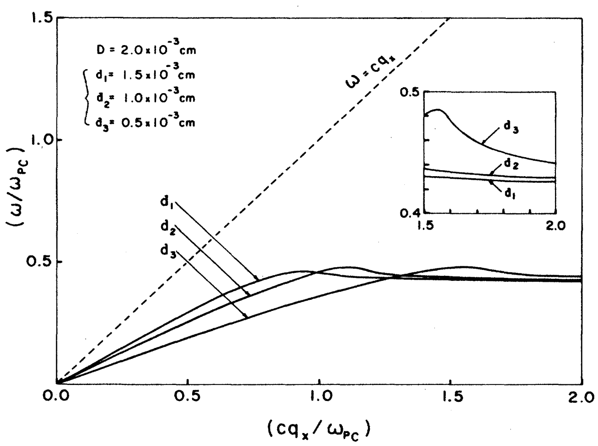

FIG. 3. Dispersion curves for the finite structure. The values of D and d are as defined in the figure. We call attention to the maxima of the respective modes, which reveal both signs of group velocity. The inset is an enlargement of the region from $cq_x/\omega_{pC}=1.5$ up to 2.0.

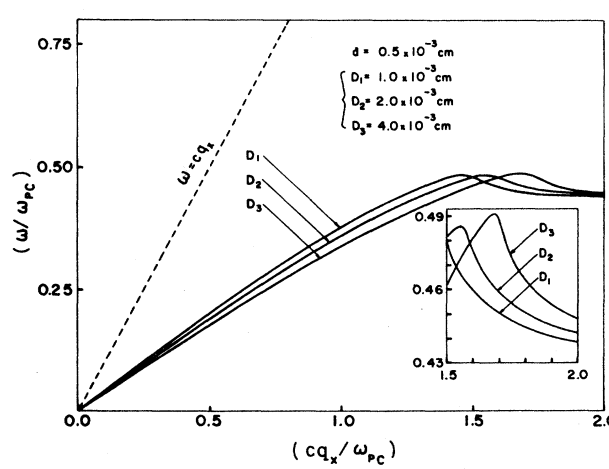

FIG. 4. Dispersion curves for the finite structure. The modes of excitations in this case are studied as a function of the size of the structure (D), keeping the insulator thickness (d) as a constant. The rest is the same as in Fig. 3.

The numerical calculations exhibit a variety of interesting features which lead us to the following conclusions. (i) For semi-infinite structure ($D \rightarrow \infty$) the frequency of CME's is directly proportional to the insulator thickness. The CME's, for all values of d, exhibit positive group velocity. For large d, the CME approaches the asymptotic limit (ω_{pC}), as is expected. We note that the dispersion curves for thinner insulator film are almost straight lines (Fig. 2). (ii) For finite structure, with D fixed (Fig. 3) the frequency is directly (inversely) proportional to the insulator thickness at low (high) wave vectors. (iii) For finite structure with constant insulator thickness (Fig. 4) the frequency of CME's is inversely (directly) proportional to the size of the structure at low (high) wave vectors. (iv) The CME's in a finite structure exhibit both (positive and negative) signs of group velocity. (v) At higher wave vectors, the CME's in a finite structure will be apparently independent of the insulator thickness (d) or the size of the structure (D), as the case may be (see Sec. IV in I).

It is worth pointing out that we studied the last case (Fig. 4) as a function of the magnitude of $\mathbf{B}_0$ at the low wave vectors in the ω-q space. It was found that the frequency of the CME increases with increasing magnetic field, just as in the perpendicular geometry.[11] Finally, a close and careful inspection reveals that the propagation characteristics of the surface excitations of a heterostructure of the type studied in the present work do not change very much from the truncated superlattice systems.[14] This remark is, however, strictly subject to the choice of the field configuration and the material parameters.

It is a pleasure to thank Professor P. Halevi for many valuable discussions. This work was supported in part by Consejo Nacional de Ciencia y Tecnológia (CONACyT), Mexico.

[1]A. B. Fowler, F. F. Fang, W. E. Howard, and P. J. Stiles, Phys. Rev. Lett. **16**, 901 (1966).

[2]F. Stern, Phys. Rev. Lett. **18**, 546 (1967).

[3]A. V. Chaplik, Zh. Eksp. Teor. Fiz. **62**, 746 (1972) [Sov. Phys.—JETP **35**, 395 (1972)].

[4]A. L. Fetter, Ann. Phys. (N.Y.) **81**, 367 (1973); **88**, 1 (1974).

[5]M. Nakayama, J. Phys. Soc. Jpn. **36**, 393 (1974).

[6]K. W. Chiu and J. J. Quinn, Phys. Rev. B **9**, 4724 (1974).

[7]A. Eguiluz, T. K. Lee, J. J. Quinn, and K. W. Chiu, Phys. Rev. B **11**, 4989 (1975).

[8]T. Ando, Solid State Commun. **27**, 895 (1978).

[9]See, for example, T. N. Theis, Surf. Sci. **98**, 515 (1980).

[10]M. S. Kushwaha, J. Appl. Phys. **60**, 2457 (1986).

[11]M. S. Kushwaha, Phys. Rev. B **35**, 3871 (1987); **37**, 1019(E) (1988); referred to as I.

[12]M. S. Kushwaha, Phys. Rev. B **36**, 4807 (1987); referred to as II.

[13]The areal density of the charge carriers is finite only in the 2D inversion layers in the x-y plane, and the applied magnetic field is oriented along the $\hat{\mathbf{x}}$ axis. This implies that nondiagonal elements $\chi^i_{xy}(i \equiv C, A)=0$ and the diagonal component χ^i_{xx} is independent of $\mathbf{B}_0$. (χ^i_{yy}, which does not appear here, is the only component which will be the function of $\mathbf{B}_0$.) One can, therefore, infer that the charge carriers in the inversion layers do not experience a magnetic force in the present configuration. As such χ^i_{xx} ($i \equiv C, A$) is given by Eq. (B1), for $\omega_C=0$, of Appendix B in I.

[14]R. F. Wallis, R. Szenics, J. J. Quinn, and G. F. Giuliani, Phys. Rev. B **36**, 1218 (1987).